3744 *J. Phys. Chem. A* **2002,** *106,* 3744−3748

Infrared Spectra and DFT Calculations for the Gold Hydrides AuH, $(H_2)AuH$, and the AuH_3 Transition State Stabilized in $(H_2)AuH_3$

Xuefeng Wang and Lester Andrews*

Department of Chemistry, University of Virginia, Charlottesville, Virginia 22904-4319

Received: November 8, 2001; In Final Form: January 4, 2002

Reactions of laser-ablated gold atoms with hydrogen (H_2, D_2, HD) in excess argon and neon and in pure deuterium produced AuH and the $(H_2)AuH$ and $(H_2)AuH_3$ complexes in increasing yields, respectively, in these matrix hosts. The diatomic molecule AuH absorbs at 2226.6 cm^{-1} in solid argon, slightly blue shifted from the gas-phase value, and the stable $(H_2)AuH$ complex appears at 2173.6 cm^{-1} on annealing to allow diffusion and association of H_2 and AuH. The higher $(H_2)AuH_3$ complex presents at 1642.0 cm^{-1} on deposition. In neon $(H_2)AuH$ and $(H_2)AuH_3$ give weak bands at 2170 and 1684 cm^{-1} with D_2 counterparts at 1559 and 1207 cm^{-1}, which become strong 1556.5 and 1198.6 cm^{-1} absorptions in pure deuterium. DFT structure and frequency calculations confirm these assignments and show that the AuH_3 transition state with an imaginary b_1 bending frequency is stabilized in the $(H_2)AuH_3$ complex with a real b_1 bending frequency observed at 457.0 cm^{-1} for $(D_2)AuD_3$.

Introduction

Gold hydride is a stable diatomic molecule that has been characterized by electronic band spectroscopy in the gas phase,[1,2] but there is no evidence for stable, solid gold hydrides.[3] Although mononuclear gold hydride complexes are either unknown or unstable,[4] gold hydrides have been observed in heterobimetallic complexes with ruthenium, iridium, and platiunum.[5−7] The anticipated AuH_3 molecule has been the subject of several recent theoretical investigations.[8−11] Gold trihydride was first predicted to be T-shaped from nonrelativistic and relativistic pseudopotential calculations.[8] Very recent quantum chemical calculations[9,10] show that the Y-shaped (H_2)-AuH complex is more stable than the T-shaped AuH_3 form. Other very recent effective core potential calculations show that AuH_3 is a transition state with an imaginary b_1 bending frequency and agree that $(H_2)AuH$ is the stable equilibrium structure.[11] Hence, it should be possible to prepare $(H_2)AuH$ from AuH in a solid matrix, and accordingly, we report the first experimental evidence for higher gold hydrides.[12] Gold is also interesting because it forms unusually strong chemical bonds due to relativistic effects.[8,13,14]

Experimental and Theoretical Methods

Laser-ablated gold atoms were reacted with H_2, D_2, and HD in excess argon and neon and with pure deuterium during condensation at 3.5 K using methods described previously for platinum and palladium hydrides and gold carbonyls.[15−17] Infrared spectra were recorded, samples were annealed and irradiated, and more spectra were recorded. Complementary density functional theory (DFT) calculations were performed using the Gaussian 98 program, BPW91 and B3LYP density functionals, 6-311++G(d,p) basis, and SDD pseudopotential.[18−22]

Results

Infrared spectra of laser-ablated gold and hydrogen reaction products in argon, neon, and deuterium matrices, and product structures and frequencies from DFT calculations will be presented in turn.

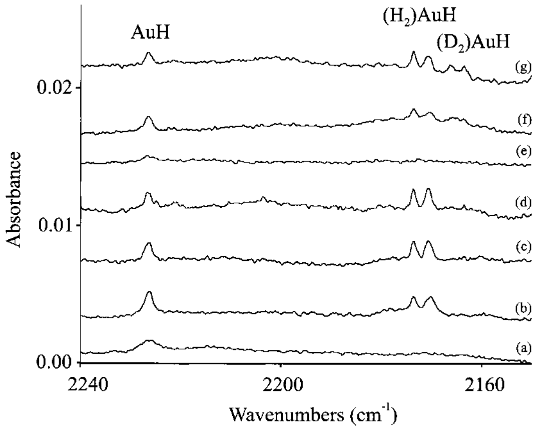

Figure 1. Infrared spectra of products of laser-ablated gold and hydrogen reactions in excess argon frozen at 3.5 K: (a) 5% H_2 in argon co-deposited for 60 min, (b) after annealing to 15 K, (c) after annealing to 20 K, (d) after annealing to 30 K, (e) 4% H_2 + 4% D_2 in argon co-deposited for 80 min, (f) after annealing to 17 K, and (g) after annealing to 25 K.

Argon. Co-deposition of laser-ablated gold atoms with H_2 in excess argon at 3.5 K produced a weak 2226.6 cm^{-1} band that increased on annealing to 15 K and then decreased on 25 K annealing while a 2173.6, 2170.6 cm^{-1} doublet is formed and increased (Figure 1). These bands shift to 1597.2 and 1559.3 cm^{-1} with D_2. In the lower region (not shown) a weak 1642.0 cm^{-1} band was not changed on 15 K annealing but disappeared on photolysis; the deuterium counterpart was observed at 1182.3 cm^{-1}.

Using $H_2 + D_2$ mixtures, the 2226.6 and 1597.2 cm^{-1} bands for AuH and AuD are unchanged, but new bands appear at 2166.2, 2163.4, and 1564.0 cm^{-1}; the upper region is also shown in Figure 1. The same 1642.0 and 1182.3 cm^{-1} bands were also observed.

---

* E-mail: lsa@virginia.edu.

10.1021/jp014105f CCC: $22.00

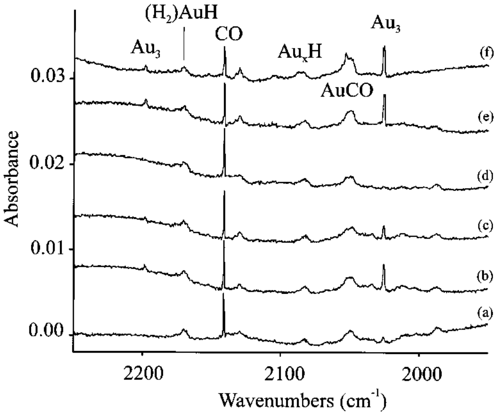

Figure 2. Infrared spectra of products of laser-ablated gold and hydrogen reactions in excess neon frozen at 3.5 K: (a) 5% H_2 in neon co-deposited for 60 min, (b) after annealing to 7 K, (c) after $\lambda > 380$ nm irradiation, (d) after $\lambda > 290$ nm irradiation, (e) after annealing to 9 K, and (f) after annealing to 11 K.

TABLE 1: Infrared Absorptions (cm^{-1}) Observed from Reactions of Gold Atoms and Dihydrogen in Excess Argon, Neon, and Deuterium

argon		neon		deuterium	
H_2	D_2	H_2	D_2	D_2	identification
2226.6					AuH
	1597.2				AuD
2173.6, 2170.6		2170.1, 2167.9			$(H_2)AuH$
	1559.3		1559.0	1556.5	$(D_2)AuD$
2076	1485	2083	1498	1493	Au_xH, Au_xD
2037.7	2037.7	2053.2	2053.2	2051	AuCO
		2025.5	2025.5		Au_3
		1986	1433		Au_xH
1642		1684			$(H_2)AuH_3$
	1182		1207	1198.6	$(D_2)AuD_3$
				1361.6	$(D_2)AuD$
				939.6	$(D_2)AuD$
				457.0	$(D_2)AuD_3$
				434.8	$(D_2)AuD$

Neon. Gold atoms with H_2 in excess neon at 3.5 K gave new product bands at 2170.1 cm^{-1} with a 2167.9 cm^{-1} shoulder (Figure 2). This band sharpened and decreased on annealing while weak bands at 2083 and 1986 cm^{-1} increased slightly and a sharp 2025.5 cm^{-1} band increased markedly on annealing. A sharp 2198.0 cm^{-1} band tracked with the 2025.5 cm^{-1} band in this and other gold experiments: these bands will be assigned to a low electronic transition of Au_3 in a later paper.[23] The 2053.2 cm^{-1} feature is due to AuCO from the trace CO impurity.[17] A weak band was observed at 1684 cm^{-1}, which decreased on annealing.

All of the above bands shifted with D_2 substitution, and the D_2 counterparts are listed in Table 1. Mixed $H_2 + D_2$ gave new features at 2163.3 and 1561.8 cm^{-1} and the same 1684 and 1207 cm^{-1} bands as observed separately with H_2 and D_2 in neon. The latter features exhibited intermediate counterparts with HD: new absorptions observed at 1831 and 1275 cm^{-1} ($A = 0.005$) decreased on annealing like the 1684 and 1207 cm^{-1} pure isotopic bands. Weak bands were also found at 2169.5 and 1561.4 cm^{-1} with HD.

Deuterium. An experiment with pure deuterium gave the rich spectrum shown in Figure 3. This spectrum is dominated by the sharp 1198.6 cm^{-1} band with 1213.7, 1212.2, and 1206.1 cm^{-1} satellites and broader features at 1556.5 and 939.6 cm^{-1}. The 1198.6 cm^{-1} band increased 20% on broadband photolysis while the 1556.5 and 939.6 cm^{-1} absorptions increased 150%. Annealing and photolysis behavior enabled a weaker 457.0 cm^{-1} band to be associated with the sharp 1198.6 cm^{-1} band and weaker 1361.6 and 434.8 bands to be grouped with the 1556.5 and 939.6 cm^{-1} absorptions.

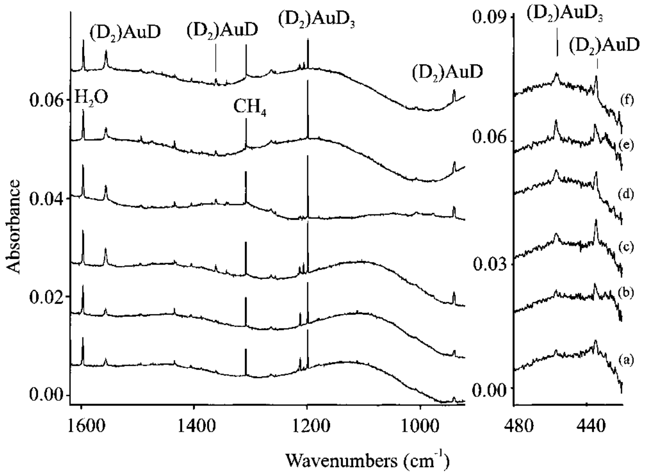

Figure 3. Infrared spectra of products of laser-ablated gold and hydrogen reactions in pure deuterium frozen at 3.5 K: (a) gold atoms co-deposited with pure deuterium for 25 min, (b) after annealing to 7 K, (c) after $\lambda > 240$ nm irradiation, (d) after annealing to 8 K, (e) after annealing to 9 K, and (f) after a second $\lambda > 240$ nm irradiation.

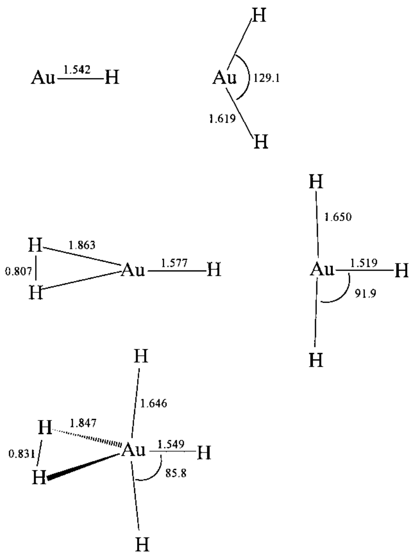

Figure 4. Structures calculated at the BPW91/6-311++G(d,p)/SDD level for gold hydrides and complexes (bond distances in angstroms, angles in degrees).

Calculations. A complete set of DFT calculations using BPW91 and B3LYP functionals was done on gold hydrides to determine frequencies and intensities for the isotopic and mixed isotopic species necessary to identify new gold hydrides prepared under matrix conditions. The two functionals gave essentially the same results as a comparison of Tables 2 and 3 shows. Structures calculated at the BPW91 level are illustrated in Figure 4. The most important new result is that the AuH_3 transition state with an imaginary b_1 frequency, the motion which converts AuH_3 to the more stable $(H_2)AuH$ form, is stabilized with virtually the same structure and Au−H stretching frequencies as in the $(H_2)AuH_3$ complex with all real frequencies. The H−Au−H′ angle is decreased from 91.9° to 85.8° and the Au−H′ bond length is increased slightly by the interaction with H_2 in the new $(H_2)AuH_3$ complex.

TABLE 2: Structures and Frequencies Calculated at the BPW91/6-311++G(d,p)/SDD Level for Gold Hydrides[a]

species	state	structure, Å, deg	frequencies, cm^{-1} (intensities, km/mol)
AuH	$^1\Sigma^+$	1.542	2250.5 (4) [1596.0 (2)][b]
AuH_2	$^2B_2$	1.619, 129.1	2003.8 (a_1, 1), 1758.0 (b_1, 1), 666.5 (a_1, 25) [1418.9 (1), 1248.7 (0), 473.4 (12)][b]
AuH_3	$^1A_1$	1.519,[c] 88.1	2405.5 (a_1, 23), 2066.8 (a_1, 0), 1846.1 (b_1, 634)
		1.650, 176.2	897.1 (a_1, 5), 854.3 (b_2, 6), 414.2i (b_1, 247)
			[1707.9 (11), 1459.5 (0), 1310.4 (318), 637.9 (2), 607.4 (3), 293.9i (124)][b]
$(H_2)AuH$	$^1A_1$	1.576	3531.2 (a_1, 0), 2192.4 (a_1, 16)
		0.807, 1.863	1268.9 (b_1, 12), 786.1 (a_1, 2), 627.2 (b_2, 2), 568.8 (b_1, 6)[c]
			[2498.1 (0), 1553.9 (8), 899.5 (6), 559.1 (1), 446.5 (1), 404.6 (3)][b]
$(H_2)AuH_3$	$^1A_1$	0.831, 1.847	3215.1 (a_1, 6), 2348.4 (a_1, 1), 2080.0 (a_1, 0)
		1.549,[c] 85.8	1865.1 (b_1, 485), 1440.8 (b_1, 16), 910.2 (a_1, 10)
		1.646, 94.2[d]	824.3 (b_2, 3), 765.2 (a_1, 2), 696.3 (b_1, 139), 673.1 (b_2, 3), 564.3 (a_2, 0), 491.9 (b_1, 13)
			[2274.7 (3), 1664.6 (1), 1471.4 (0), 1325.6 (241), 1019.9 (9), 644.3 (5), 585.8 (1), 546.4 (1), 493.7 (71), 479.4 (2), 399.2 (0), 349.4 (6)][b]

[a] All C_{2v} symmetry but AuH. [b] Deuterium counterparts in square brackets. [c] Unique shorter Au−H bond. [d] Airplane structure with $(H_2)Au$ perpendicular to AuH_3 plane.

TABLE 3: Structures and Frequencies Calculated at the B3LYP/6-311++G(d,p)/SDD Level for Gold Hydrides[a]

species	state	structure, Å, deg	frequencies, cm^{-1} (intensities, km/mol)
AuH	$^1\Sigma^+$	1.546	2227.4 (15) [1579.6 (8)][b]
AuH_2	$^2B_2$	1.619, 128.6	1995.2 (a_1, 2), 1742.1 (b_1, 1), 666.5 (a_1, 23) [1412.8 (1), 1237.4 (0.3), 473.4 (17)][b]
AuH_3	$^1A_1$	1.515,[c] 87.9	2425.0 (a_1, 17), 2096.1 (a_1, 0), 1859.9 (b_1, 704)
		1.646, 184.2	905.1 (a_1, 7), 861.5 (b2, 9), 374.8i (b_1, 282)
			[1719.7 (8), 1482.7 (0), 1322.5 (354), 643.4 (4), 612.2 (5), 265.5i (141)][b]
$(H_2)AuH$	$^1A_1$	1.574	3778.3 (a_1, 4), 2205.9 (a_1, 26)
		0.787, 1.902	1185.0 (b_1, 11), 702.4 (a_1, 4), 607.9 (b2, 6), 556.0 (b_1, 11)
			[2672.8 (2), 1563.7 (13), 839.1 (5), 499.5 (2), 432.7 (3), 395.4 (6)][b]
$(H_2)AuH_3$	$^1A_1$	0.805, 1.887	3520.5 (a_1, 0), 2389.8 (a_1, 1), 2104.1 (a_1, 0)
		1.540,[c] 86.0	1873.2 (b_1, 558), 1361.0 (b_1, 18), 887.9 (a_1, 10)
		1.643, 94.0[d]	837.5 (b_2, 6), 763.5 (a_1, 1), 704.3 (b_1, 163), 656.1 (b_2, 1), 538.1 (a_2, 0), 497.8 (b_1, 12)
			[2490.5 (0), 1694.1 (1), 1488.4 (0), 1331.6 (278), 963.4 (10), 621.1 (5), 595.0 (3), 545.5 (1), 499.2 (83) , 467.4 (1), 380.6 (0), 353.6 (6)][b]

[a] All C_{2v} symmetry but AuH. [b] Deuterium counterparts in square brackets. [c] Unique shorter Au−H bond. [d] Airplane structure with $(H_2)Au$ perpendicular to AuH_3 plane.

Discussion

The gold hydride species will be identified based on isotopic substitution, comparison of argon, neon, and deuterium matrix results, and DFT calculations.

AuH. The 2226.6 and 1597.2 cm^{-1} bands observed with laser-ablated gold atoms and H_2 and D_2 in solid argon are slightly blue shifted from the 2218.8 and 1591.7 cm^{-1} fundamentals deduced for AuH and AuD from electronic band spectra.[1,2] Both data sets have the 1.394 H/D frequency ratio, which is appropriate for a heavy metal hydride vibration. The 2226.6 and 1597.2 cm^{-1} bands are invariant with HD reagent, which shows that one H or D atom is involved in the vibration. Accordingly, the 2226.6 and 1597.2 cm^{-1} bands are assigned to the AuH and AuD diatomic molecules in solid argon. Evidence for the formation of H atoms in these experiments is found in the detection of HO_2 and Ar_nH^+ species.[25] These diatomic molecules are not trapped in solid neon owing to diffusion of H_2 and D_2 and reaction to form higher hydrides. In pure deuterium, reaction to form higher deuterides is immediate.

(H_2)AuH. A sharp 2173.6, 2170.6 cm^{-1} doublet in argon appears and increases on annealing to allow diffusion of H_2 at the expense of AuH. A single band at 1559.3 cm^{-1} increases on annealing to allow diffusion of D_2 at the expense of AuD. Our DFT calculations predict the strongest Au−H stretching mode for $(H_2)AuH$ 56.8 cm^{-1} (BPW91) and 21.5 cm^{-1} (B3LYP) below AuH and with greater infrared intensity. The H/D frequency ratio 1.394 is the same as for AuH/AuD. The bands shift slightly to 2170.1 and 1559.0 cm^{-1} in neon.

Assignment of those bands to the Au−H stretching mode of the stable $(H_2)AuH$ molecule[10,11] is further substantiated by observation of three fundamentals and a combination band in the pure deuterium matrix where the yield of $(D_2)AuD$ is increased owing to the effectively high concentration of the D_2 reagent. The 1556.5, 939.6, and 434.8 cm^{-1} bands with 0.0037, 0.0024, and 0.005 absorbances (Figure 3c) are in very good agreement with the BPW91 predictions of 1553.9 (8), 898.5 (6), and 404.6 cm^{-1} (3 km/mol), except the lowest mode is more intense than calculated. The weaker 1361.6 cm^{-1} absorption is due to a combination of b_1 fundamentals ($939.6 + 434.8 = 1374.4$), where the sum of fundamentals slightly exceeds the combination band because of anharmonicity. The observation of a combination band supports the assignment of fundamentals to $(D_2)AuD$. Unfortunately, the D−D stretching fundamental calculated at 2498.1 cm^{-1} BPW91 with zero intensity could not be observed.

Mixed isotopic spectra further support this assignment. First, HD in neon gave 2169.5 and 1561.4 cm^{-1} bands, down from 2170.1 cm^{-1} for $(H_2)AuH$ and up from 1559.0 for $(D_2)AuD$. Our BPW91 calculations predict 1.8 and 3.8 cm^{-1}, respectively, for these separations for (HD)AuH and (HD)AuD. Second, $H_2 + D_2$ in neon gave the above pure isotopic frequencies plus new 1562.0 and 2163.3 cm^{-1} bands. Our BPW91 calculations predict 6.5 and 5.4 cm^{-1} separations, respectively, for $(D_2)AuH$ and for $(H_2)AuD$. Third, $H_2 + D_2$ in argon gave the spectrum shown in Figure 1: the 2226.6 cm^{-1} AuH band and the sharp 2173.6, 2170.6 cm^{-1} doublet plus a new 2166.0, 2163.4 cm^{-1} doublet. The new doublet shifts down 7.6, 7.2 cm^{-1} for $(D_2)AuH$. An analogous 1564.0 cm^{-1} band was observed for $(H_2)AuD$ above $(D_2)AuD$ at 1559.3 cm^{-1}.

$(H_2)AuH_3$. The strong, sharp 1198.6 cm^{-1} absorption in pure deuterium and the weaker 1642.0, 1182.3 cm^{-1} argon and 1684, 1207 cm^{-1} neon H_2 and D_2 counterparts are in reasonable agreement with the DFT prediction of a very strong b_1 antisymmetric H−Au−H stretching mode for AuH_3. However, AuH_3 is less stable than $(H_2)AuH$ (26−28 kcal/mol higher at CCSD(T) level)[10,11] and AuH_3 is a transition state with an imaginary b_1 antisymmetric bending mode. In the argon matrix where a wide range of annealing temperature is available, the 1642.0, 1182.4 cm^{-1} bands decrease on annealing while the $(H_2)AuH$ absorption increases. Calculations were performed to find a stable complex of AuH_3 that might match the observed spectrum. The Ne_2AuH_3 complex decomposed; however, $(H_2)AuH_3$ is stable to dissociation to H_2 and AuH_3 (7.9 kcal/mol, B3LYP; 9.2 kcal/mol, BPW91) but higher than $H_2 + (H_2)AuH$ (22.8 kcal/mol, B3LYP; 18.6 kcal/mol, BPW91). There is apparently a considerable energy barrier for $(H_2)AuH_3$ to eliminate H_2 that is at least as high as the above 7.9 or 9.2 kcal/mol binding energies.

The three Au−H stretching modes in the AuH_3 transition state are changed little in the stable $(H_2)AuH_3$ complex, but the imaginary b_1 bending frequency involving the unique, short Au−H bond is real, increased by 68−88%, and has significant infrared intensity in $(H_2)AuH_3$ using BPW91 and B3LYP functionals. Thereby the AuH_3 transition state is stabilized: its imaginary b_1 mode is eliminated in the dihydrogen complex. The first-given above absorptions are assigned to the strong b_1 antisymmetric H−Au−H stretching mode for $(H_2)AuH_3$. In the pure deuterium experiment the new 457.0 cm^{-1} band is half the intensity of the 1198.6 cm^{-1} band, and it is assigned to the above-described b_1 bending mode. DFT calculations (Tables 2, 3) predict these strong b_1 modes at 493.7, 499.2, and 1325.6, 1331.6 cm^{-1} with 1:3 relative intensity, which is in very good agreement with the bands observed in pure deuterium.

Mixed isotopic spectra support this identification of $(H_2)AuH_3$. First, HD in neon gave two new bands at 1831 and 1275 cm^{-1}, which decreased on annealing as did the 1684 and 1207 cm^{-1} pure isotopic bands. Our BPW91 calculations predict absorptions for both $(H_2)AuHDH$ and $(H_2)AuHDD$ 120 and 59 cm^{-1} higher than the strong pure isotopic bands; the new bands 147 and 68 cm^{-1} higher are in good agreement. Note that vibrations involving the two equivalent longer Au−H bonds do not couple with the shorter almost orthogonal Au−H bond. Second, $H_2 + D_2$ in neon and argon gave both pure isotopic bands and no new features. Our BPW91 calculations predict a 0.1 cm^{-1} shift for $(H_2)AuH_2H$ and $(H_2)AuH_2D$ and a small (0.6 cm^{-1}) shift for $(D_2)AuH_3$, and no shift is observed in these bands (1.2 cm^{-1} half-width). Third, HD in argon gave weak bands at 1798 and 1252 cm^{-1} that are due to both $(H_2)AuHDH$ and $(H_2)AuHDD$ complexes as discussed above.

Reaction Mechanisms. The first step in these reactions is to provide excess energy to promote endothermic (29.0 kcal/mol)[1] reaction 1. Gold hydrides are typically investigated in electrical discharges with hot (1700 °C) metal vapor,[2] which can both excite gold atoms and dissociate molecular hydrogen. Here laser-ablated gold atoms have sufficient excess energy[26] to drive reaction 1. The small growth of AuH on first annealing is due to Au + H atom combination as H(D) atoms are manifested in trace quantities of other species.[24,25] The $(H_2)AuH$ complex is formed spontaneously in exothermic (−5.7 kcal/mol, B3LYP; −6.2 kcal/mol, BPW91; −13 kcal/mol, CCSD(T)[10]) reaction 2 on annealing the argon matrix to allow diffusion of H_2.

Collision of energetic AuH molecules from reaction 1 and H_2 during sample deposition can form the AuH_3 transition state (26−28 kcal/mol higher than $(H_2)AuH$ at the CCSD(T) level),[10,11] reaction 3,which would rearrange to $(H_2)AuH$ if not stabilized by an additional dihydrogen in the trihydride complex, reaction 4.

$$Au(^2S) + H_2(^1\Sigma_g^{\ +}) \rightarrow AuH(^1\Sigma^+) + H(^2S) \qquad (1)$$

$$H_2 + AuH \rightarrow (H_2)AuH \qquad (2)$$

$$AuH^* + H_2 \rightarrow (AuH_3)^* \rightarrow (H_2)AuH \qquad (3)$$

$$H_2 + (AuH_3)^* \rightarrow (H_2)AuH_3 \qquad (4)$$

The $(H_2)AuH_3$ complex is stable; apparently activation energy is required to break two Au−H bonds and eliminate H_2 to form $(H_2)AuH$, which is more stable by 18.6 kcal/mol (BPW91) or 22.8 kcal/mol (B3LYP). It is therefore clear why the yield of $(D_2)AuD_3$ is relatively high on deposition of laser-ablated gold atoms in the pure deuterium matrix. It is interesting to note that no evidence of gold deuteride was found for sputtered gold atoms in pure deuterium at 4.2 K.[27] Apparently, the sputtered gold atoms do not have sufficient excess energy to form gold deuteride via endothermic reaction 1.

The contrasting yields of the three gold hydride species in argon, neon, and deuterium matrix experiments depend on condensation rate at 3.5 K and the effective concentration of the $H_2(D_2)$ reagent. In argon AuH is isolated from H_2 on deposition but not in the more slowly condensing neon medium. Deuterium serves as both a reactive and an inert matrix to produce and stabilize gold deuteride complexes with little perturbation.[28]

Conclusions

Reactions of laser-ablated gold atoms with hydrogen (H_2, D_2, HD) in excess argon and neon and in pure deuterium produced AuH and the $(H_2)AuH$ and $(H_2)AuH_3$ complexes in increasing yields, respectively, in these matrix hosts. The diatomic molecule AuH absorbs at 2226.6 cm^{-1} in solid argon, slightly blue shifted from the gas-phase value, and the stable $(H_2)AuH$ complex appears at 2173.6 cm^{-1} on annealing to allow diffusion and association of H_2 and AuH; the higher $(H_2)AuH_3$ complex presents at 1642.0 cm^{-1} on deposition. In neon $(H_2)AuH$ and $(H_2)AuH_3$ give weak bands at 2170 and 1684 cm^{-1} with D_2 counterparts at 1559 and 1207 cm^{-1}, which become strong 1556.5 and 1198.6 cm^{-1} absorptions in pure deuterium. DFT structure and frequency calculations confirm these assignments and show that the AuH_3 transition state with an imaginary b_1 bending frequency is stabilized in the $(H_2)AuH_3$ complex with a real b_1 bending frequency observed at 457.0 cm^{-1} for $(D_2)AuD_3$.

Acknowledgment. We gratefully acknowledge support for this work from NSF Grant CHE 00-78836.

References and Notes

(1) Huber, K. P.; Herzberg, G. *Molecular Spectra and Molecular Structure. IV. Constants of Diatomic Molecules*; Van Nostrand Reinhold: New York, 1979.

(2) Hulthen, E.; Zumstein, R. V. *Phys. Rev.* **1926**, *28*, 13. Ringström, U. *Nature* **1963**, *198*, 981; *Ark. Fys.* **1966**, *32*, 19.

(3) Wiberg, E.; Neumaier, H. *Inorg. Nucl. Chem. Lett.* **1965**, *1*, 35.

(4) Lehner, H.; Matt, D.; Pregosin, P. S.; Venanzi, L. M.; Albinati, A. *J. Am. Chem. Soc.* **1982**, *104*, 6825.

(5) Alexander, D. B.; Johnson, B. J.; Johnson, S. M.; Casalnuovo, A. L.; Pignolet, L. H. *J. Am. Chem. Soc.* **1986**, *108*, 4409.

(6) Albinati, A.; Lehner, H.; Venanzi, L. M.; Wolfer, M. *Inorg. Chem.* **1987**, *26*, 3933.

(7) Albinati, A.; Anklin, C.; Janser, P.; Lehner, H.; Matt, D.; Pregosin, P. S.; Venanzi, L. M. *Inorg. Chem.* **1989**, *28*, 1105.

(8) Schwerdtfeger, P.; Boyd, P. D. W.; Brienne, S.; Burrell, A. K. *Inorg. Chem*. **1992**, *31*, 3411 and references therein.

(9) Bayse, C. A.; Hall, M. B. *J. Am. Chem. Soc*. **1999**, *121*, 1348.

(10) Bayse, C. A. *J. Phys. Chem. A* **2001**, *105*, 5902.

(11) Balabanov, N. B.; Boggs, J. E. *J. Phys. Chem. A* **2001**, *105*, 5906.

(12) Wang, X.; Andrews, L. *J. Am. Chem. Soc.* **2001**, *123*, 12899.

(13) Declaux, J. P.; Pyykkö, P. *Chem. Phys. Lett.* **1976**, *39*, 300.

(14) (a) Pyykkö, P. *J. Am. Chem. Soc.* **1995**, *117*, 2067. (b) Schröder, D.; Schwarz, H.; Hrušák, J.; Pyykko, P. *Inorg. Chem.* **1998**, *37*, 624.

(15) Andrews, L.; Wang, X.; Manceron, L. *J. Chem. Phys.* **2001**, *114*, 1559.

(16) (a) Andrews, L.; Manceron, L.; Alikhani, M. E.; Wang, X. *J. Am. Chem. Soc.* **2000**, *122*, 11011. (b) Andrews, L.; Wang, X.; Alikhani, M. E.; Manceron, L. *J. Phys. Chem. A* **2001**, *105*, 3052.

(17) Liang, B.; Andrews, L. *J. Phys. Chem. A* **2000**, *104*, 9156.

(18) Frisch, M. J.; Trucks, G. W.; Schlegel, H. B.; Scuseria, G. E.; Robb, M. A.; Cheeseman, J. R.; Zakrzewski, V. G.; Montgomery, J. A., Jr.; Stratmann, R. E.; Burant, J. C.; Dapprich, S.; Millam, J. M.; Daniels, A. D.; Kudin, K. N.; Strain, M. C.; Farkas, O.; Tomasi, J.; Barone, V.; Cossi, M.; Cammi, R.; Mennucci, B.; Pomelli, C.; Adamo, C.; Clifford, S.; Ochterski, J.; Petersson, G. A.; Ayala, P. Y.; Cui, Q.; Morokuma, K.; Malick, D. K.; Rabuck, A. D.; Raghavachari, K.; Foresman, J. B.; Cioslowski, J.; Ortiz, J. V.; Baboul, A. G.; Stefanov, B. B.; Liu, G.; Liashenko, A.; Piskorz, P.; Komaromi, I.; Gomperts, R.; Martin, R. L.; Fox, D. J.; Keith, T.; Al-Laham, M. A.; Peng, C. Y.; Nanayakkara, A.; Gonzalez, C.; Challacombe, M.; Gill, P. M. W.; Johnson, B.; Chen, W.; Wong, M. W.; Andres, J. L.; Gonzalez, C.; Head-Gordon, M.; Replogle, E. S. and Pople, J. A. *Gaussian 98*, Revision A.7; Gaussian, Inc.: Pittsburgh, PA, 1998.

(19) (a) Becke, A. D. *J. Chem. Phys.* **1993**, *98*, 5648. (b) Lee, C.; Yang, W.; Parr, R. G. *Phys. Rev. B* **1988**, *37*, 785.

(20) (a) Becke, A. D. *Phys. Rev. A* **1988**, *38*, 3098. (b) Perdew, J. P.; Wang, Y. *Phys. Rev. B* **1992**, *45*, 13244.

(21) (a) Krishnan, R.; Binkley, J. S.; Seeger, R.; Pople, J. A. *J. Chem. Phys.* **1980**, *72*, 650. (b) Frisch, M. J.; Pople, J. A.; Binkley, J. S. *J. Chem. Phys.* **1984**, *80*, 3265.

(22) Andrae, D.; Haussermann, U.; Dolg, M.; Stoll, H.; Preuss, H. *Theor. Chim. Acta* **1990**, *77*, 123.

(23) Guo, R.; Balasubramanian, K.; Wang, X.; Andrews, L. To be published.

(24) Millgan, D. E.; Jacox, M. E. *J. Chem. Phys.* **1963**, *38*, 2627. Smith, D. W.; Andrews, L. *J. Chem. Phys.* **1974**, *60*, 81.

(25) Milligan, D. E.; Jacox, M. E. *J. Mol. Spectrosc.* **1973**, *46*, 460. Wight, C. A.; Ault, B. S.; Andrews, L. *J. Chem. Phys*. **1976**, *65*, 1244.

(26) Kang, H.; Beauchamp, J. L. *J. Phys. Chem*. **1985**, *89*, 3364.

(27) Goven, D. M.; Bates, J. K. *Inorg. Chem.* **1977**, *16*, 2450.

(28) Van Zee, R. J.; Li, S.; Weltner, W., Jr. *J. Chem. Phys.* **1995**, *102*, 4367.